ISSN 1392–1207. MECHANIKA. 2017 Volume 23(2): 182–189

Experimental and numerical analysis of flexural concrete-UHPFRC/RC composite members

T. Zingaila*, M. Augonis, M.R.T. Arruda***, E. Šerelis****, Š. Kelpša*******
**Kaunas University of Technology, Studentų 48, 51367 Kaunas, Lithuania, E-mail: tadas.zingaila@ktu.lt*
***Kaunas University of Technology, Studentų 48, 51367 Kaunas, Lithuania, E-mail: mindaugas.augonis@ktu.lt*
**** University of Lisbon, Instituto Superior Técnico CERIS-ICIST, Av. Rovisco Pais 1, 1049-001, Lisbon, Portugal, E-mail: mario.rui.arruda@tecnico.ulisboa.pt*
*****Kaunas University of Technology, Studentų 48, 51367 Kaunas, Lithuania, E-mail: evaldas.serelis@ktu.lt*
******Kaunas University of Technology, Studentų 48, 51367 Kaunas, Lithuania, E-mail: sarunas.kelpsa@ktu.lt*

crossref http://dx.doi.org/10.5755/j01.mech.23.2.17210

1. Introduction

The efficiency of existing reinforced concrete structures strengthening with ultra-high performance fibre reinforced concrete (UHPFRC) have been studied by many authors [1-7]. However, not enough investigations are directly concentrated on experimental and theoretical analysis of newly cast concrete-UHPFRC/RC members structural behaviour [8, 9]. Relatively high price of UHPFRC sets a limits to carry out experimental analysis, especially in less developed countries. Due to this reason numerical and analytical calculation models of composite flexural members have to be fully analysed, safe to use, and to be as simple as possible for practical application. For this purpose, many research has to be carried out for clear understanding of composite members structural behaviour. Contribution of every scientist to this topic is very important.

Mechanical properties of ordinary concrete can be found in European design standard [10], national technical regulations, design codes [11, 12] and can be safely used for design of reinforced concrete structures. However, UHPFRC has only interim design recommendations [13], which does not present classification by compressive strength class as it is clearly done for ordinary concrete. However, in contrast to concrete, the tensile response of UHPFRC takes more important role on structural behaviour of flexural reinforced concrete members. Depending on such factors as mix components, amount of steel fibres, technological difficulties, this type of concrete has large variety on tensile strength and post-peak response. Direct uniaxial tensile tests have not been standardised and are difficult to carry out, therefore various inverse analysis methods [13, 14] have been made for this purpose and applied for uniaxial tensile response determination from more simple tests. Various tensile test setups can be found in literature [15, 16]. All these problems determine large variety of tensile properties, which make significant contribution in additional inaccuracies of results of analytical and numerical structural behaviour calculations. Standardised documents with tensile response classification would help to minimize errors due to the influence of inaccurate mechanical properties.

As it was observed in previous studies [1-9], reinforced concrete beams strengthened or newly cast with additional UHPFRC layer in tension zone of the member can exhibit better structural performance. Application of UHPFRC determines enhanced flexural and shear capacity, increased stiffness, reduced crack widths and spacing, delayed formation of localized macrocracks, also it serves as protection function for reinforcement due to its low water permeability [3, 8].

Numerical analysis of UHPFRC beams can be found in scientific papers [17-20]. Comparison of numerical and experimental results showed that finite element (FE) method is capable for predicting UHPFRC flexural members structural behaviour. Concrete damaged plasticity (CDP) [21] model given in FE software ABAQUS is suitable for concrete and UHPFRC. However, comparing different scientific papers [17-20] can be found different parameters describing concrete plasticity. Furthermore, it can be observed that it is usual to use stress-strain relation of tensile concrete, which influences on increased mesh dependency. ABAQUS provides post-failure stress-displacement relation for tension concrete, which can be defined by post-failure stress and crack displacement relation in tabular form or specified by fracture energy directly as a material property [22]. This would help to predict the tensile post-failure model which would be suitable for numerical analysis with minimized mesh dependency. Fracture energy of ordinary concrete can be calculated using the methodology presented in CEB/FIP model codes [11, 12]. It is necessary to emphasize that older and new model codes give different values of fracture energy. For UHPFRC fracture energy can be determined from experimental tests or calculated according to already suggested methods [16, 23, 24]. However, due to different mix compositions, fibre type and volume percent, these methods have some limitations, and it is necessary to determine its applicability to structural members.

Numerical analysis of flexural concrete-UHPFRC/RC composite members requires moreover knowledge for prediction of its structural response. In some cases, additional attention should be paid to interface modelling between different composites. This paper is intended for deformational analysis of newly cast flexural concrete-UHPFRC/RC composite members. Experimental and numerical analysis is carried out and the results are compared.

2. Experimental investigations

2.1. Test programme

Experimental investigations were carried out on purpose to determine the structural behaviour of flexural

concrete-UHPFRC/RC composite members. Test programme consisted of concrete, UHPFRC and steel reinforcement properties characterisation tests and determination of structural behaviour of 6 intermediate-scale beams using 4-point bending tests (Fig. 1).

Fig. 1 Test setup of concrete-UHPFRC/RC composite beam

2.2. Mixtures and material properties

Two different mix compositions were used in experimental program. Mix composition for concrete is given in Table 1, and UHPFRC mixture is presented in Table 2.

Table 1

Mix composition of high strength concrete

Materials	Quantity, kg/m^3
CEM I 42.5 R	360
Water	150
Coarse aggregate (gravel 4/16 fr.)	922
Fine aggregate (sand 0/4 fr.)	907
Superplasticizer	2.16

Table 2

Mix composition of ultra-high performance concrete

Materials	Quantity, kg/m^3
CEM I 52.5 R	735
Water	158
SiO_2 powder	99
Glass powder	412
Quartz sand (0/2 fr.)	962
Superplasticizer	36.76
Straight steel fibres 13/0.2 (2% by vol.)	157

Concrete and UHPFRC properties characterisation tests were carried out at the age of 28 days. Average values of mechanical properties are presented in Table 3. Tensile strength of concrete and UHPFRC were measured indirectly, from flexural tensile strength tests.

Table 3

Mechanical properties of concrete and UHPFRC

Average values of mechanical properties	MPa
Concrete (HSC)	
Cylindrical compressive strength, f_{cm}	51.8
Tensile strength, f_{ctm}	3.84
Secant modulus of elasticity, E_{cm}	33380
UHPFRC	
Cubical compressive strength, $f_{cm,100}$	138.2
Flexural tensile strength, $f_{ctm,fl}$	11.59
Secant modulus of elasticity, E_{cm}	44390

All beams were reinforced with the same rebar cages, grade B500B. Longitudinal bottom reinforcement ø14 mm, top reinforcement ø10 mm and shear reinforcement ø8 mm. Average yielding strength f_{sy} = 565.4 MPa and ultimate strength f_{su} = 652.4 MPa, modulus of elasticity E_s = 200 GPa.

In present study straight steel fibres (2% by volume) with tensile strength $f_{fb,u}$ = 2750 MPa were used only for UHPFRC mixture. Fibre length l_f = 13 mm, diameter d_f = 0.21 mm, aspect ratio l_f / d_f = 62, modulus of elasticity $E_{fb,s}$ = 200 GPa.

2.3. Specimens and test setup

Test setup of reinforced concrete beams and concrete-UHPFRC/RC composite beams are shown in Fig. 4. In total, four concrete-UHPFRC/RC composite beams were cast and tested in experimental program. In order to determine the effectiveness of composite beams, two rectangular cross-section RC beams were cast additionally. Beams types and properties are given in Fig. 2 and Table 4.

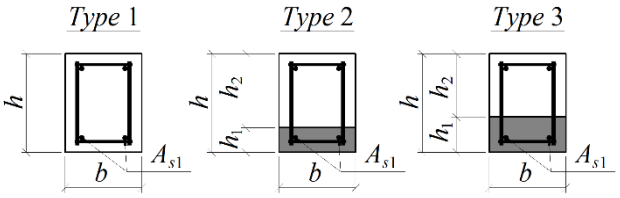

Fig. 2 Beams cross-section types

Table 4

Beams cross-section properties

Beam type	Beam description	h, mm	h_1/h_2, mm	b, mm	A_{s1}, mm^2
Type1	B1-200-2d14	198	–	159	308
Type1	B2-200-2d14	199	–	160	308
Type2	B3-50/150-2d14	199	49/150	159	308
Type2	B4-50/150-2d14	198	48/150	160	308
Type3	B5-70/130-2d14	199	70/129	159	308
Type3	B6-70/130-2d14	199	69/130	161	308

In the middle of the beams strain gauges were installed to measure the strains in top and bottom rebars. Special covering tape was used to protect strain gauges from mechanical damage and water. Additional steel rebars were welded in both sides of strain gauges in order to compensate the bond loss, which was done in the zone of covering tape. The cables of strain gauges were put out through the frameworks and during the testing of beams the cables were connected to strain measuring equipment. Prepared rebar cages are shown in Fig. 3.

Fig. 3 Strain gauges installed on rebar cages and protected by special covering tape

The experiments were carried out on purpose to

simulate the production of new concrete-UHPFRC/RC flexural composite beams. Considering to concrete and UHPFRC mix properties and workability, it was chosen to cast the beams upside down and start casting from concrete layer. Vibro table was used to compact the concrete mix. After that the second layer of UHPFRC was cast and full beam vibrated on vibro table. The time between casting phases was minimised in order to achieve the best bond conditions in the interface zone between concrete and UHPFRC.

The ends of longitudinal rebar were welded to perpendicular anchoring steel rebar in order to avoid slip during loading and guarantee good anchorage (see Fig. 4).

Three digital indicators were used to measure the deformations at the mid-span of the beam and at the supports. Using these measurements, the clear deflection of the beams was calculated. Scheme of digital indicators arrangement is presented in Fig. 4.

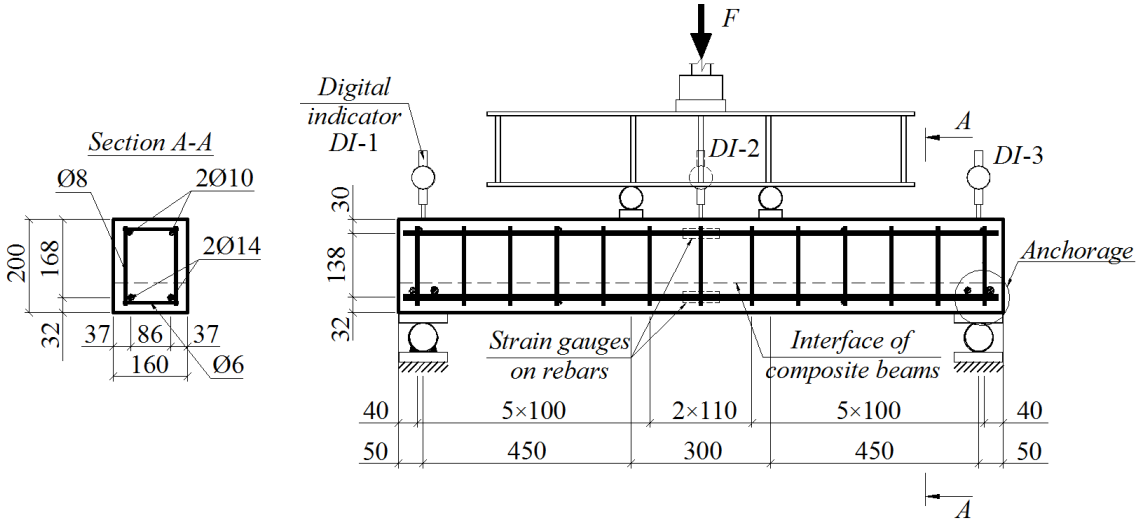

Fig. 4 Test setup and details of RC beams and concrete-UHPFRC/RC composite beams

3. Numerical investigations

3.1. FE model description

Numerical analysis of tested beams was carried out using FE software ABAQUS, in which a physically non-linear analysis was taken into account modelling concrete-UHPFRC/RC composite beams. This software have been tested with ordinary RC structures and also with UHPFRC [8, 17, 25, 26].

3-dimensional model was created for composite beams numerical analysis. Eight-node linear brick (C3D8) elements were used for concrete, UHPFRC, steel plates at the support and for load cell. Two-node linear 3-D truss (T3D2) elements were used to create longitudinal and shear reinforcement. All types of reinforcement were embedded in concrete and UHPFRC. Perfect bond between steel and concrete (UHPFRC), as well as concrete and UHPFRC was assumed. Fully constrained contact behaviour was defined using surface-based tie constraints. All beams were loaded by displacement control in vertical direction. Initially a mesh dependency test was performed, and after some calibrations 25 mm structured mesh size was chosen for the calculation. In order to reduce the computational cost, a symmetrical analysis was performed, in both longitudinal and transversal axes.

3.2. Material models

CDP model was chosen for modelling concrete and UHPFRC materials. This model uses concepts of isotropic damaged elasticity together with isotropic tensile and compressive plasticity. Furthermore, it can be used for plain concrete and reinforced concrete structures [22].

Stress-strain relation of compressive concrete which is given in ABAQUS is presented in Fig. 5. and can be described using equation (1) [22]:

$$\sigma_c = (1-d_c)E_0\left(\varepsilon_c - \tilde{\varepsilon}_c^{pl}\right), \tag{1}$$

where d_c is damage variable of compressive concrete; E_0 is initial (undamaged) elastic stiffness of concrete; ε_c is strain of compressive concrete; $\tilde{\varepsilon}_c^{pl}$ is equivalent plastic strain of compressive concrete.

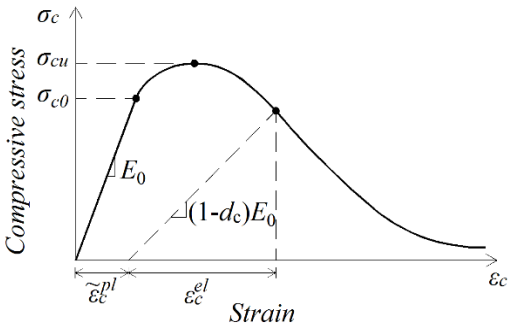

Fig. 5 Response of concrete to uniaxial loading in compression

Until the crack opening linear stress-stain relation is used for tensile concrete and UHPFRC. On purpose to avoid mesh dependency as much as possible in FE model, post-failure tensile stress-displacement relation (Fig. 6) and tensile stress-fracture energy relation (Fig. 7) were used instead of stress-strain relation.

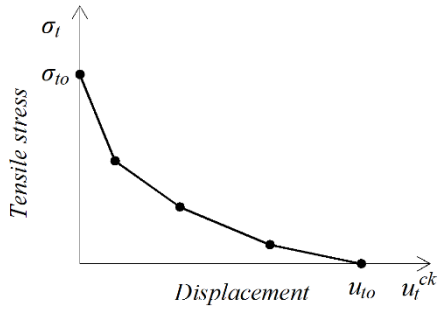

Fig. 6 Post-failure stress-displacement relation in tension

Decreasing branch of tensile ordinary concrete was calculated according to methodology given in CEB/FIP Model Code 2010 (Eqs. 2 and 3).

$$\sigma_{ct} = f_{ctm}\left(1-0.8\frac{w}{w_1}\right) \text{ for } w \le w_1\,; \tag{2}$$

$$\sigma_{ct} = f_{ctm}\left(0.25-0.05\frac{w}{w_1}\right) \text{ for } w_1 < w \le w_c\,, \tag{3}$$

where w is crack opening in mm; w_1 is G_f / f_{ctm} in mm when $\sigma_{ct} = 0.20\, f_{ctm}$; w_c is $5\, G_f / f_{ctm}$ in mm when $\sigma_{ct} = 0$; G_f is fracture energy in N/mm; f_{ctm} is mean value of tensile strength in MPa.

For UHPRFC decreasing branch was described as post-failure stress-fracture energy (G_f) relation (Fig. 7).

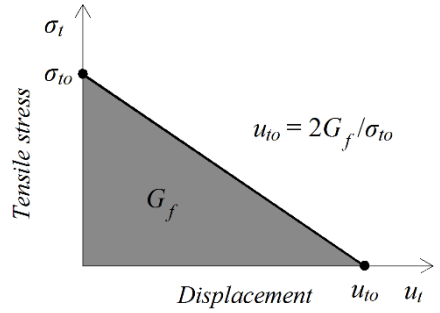

Fig. 7 Post-failure stress-fracture energy relation in tension

Properties of reinforcement was described as bi-linear stress-strain relation (Fig. 8).

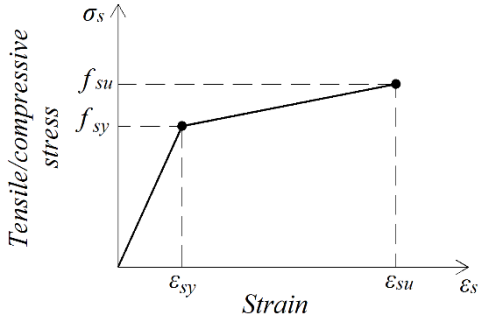

Fig. 8 Bi-linear stress-strain relation of reinforcement in tension and compression

4. Experimental and numerical results

4.1. Effectiveness of concrete-UHPFRC/RC beams

The analysis of load-deflection relationship was limited to the maximum load at about the beginning of reinforcement yielding point, as it is usual case in the design of reinforced concrete structures. It can be clearly seen from Fig. 9 that UHPFRC layer in tension zone has positive effect on concrete-UHPFRC/RC composite beams structural performance in comparison to RC beams.

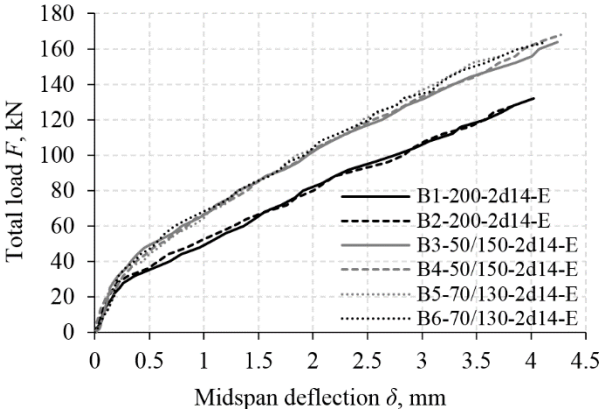

Fig. 9 Experimentally measured deflection at midspan

After the crack opening high amount of small steel fibres has a significant role on crack propagation. Instead of wide and rarely distributed cracks, it is fine and more densely distributed ones (Fig. 10), which determines stiffer structural behaviour of composite members.

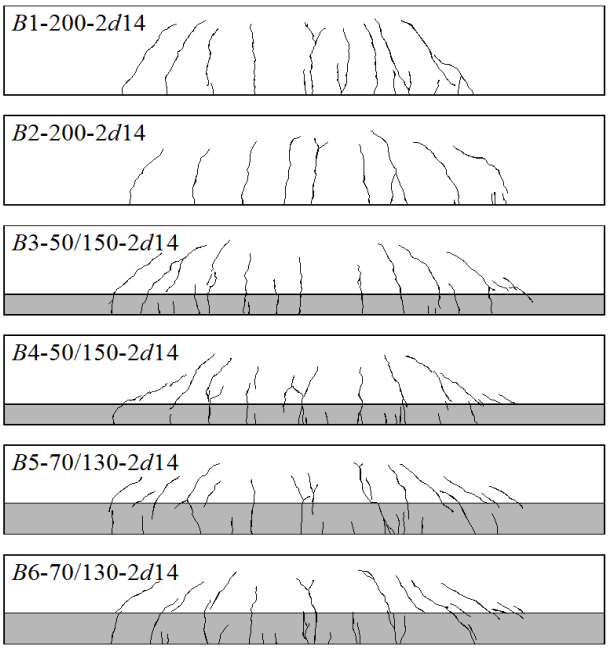

Fig. 10 Cracking patterns of different type of tested beams at failure load

The tensile force is transferred by reinforcement and steel fibres, therefore yielding of reinforcement is reached at higher loads. Steel fibres are very strong (tensile strength $f_{fb,u}$ = 2750 MPa) and short (13 mm), therefore it is pulled out from concrete matrix due to not enough anchorage length. This determines many fine and densely distributed cracks. However, for UHPFRC/RC flexural members with high amount of steel fibres more intense multiple cracking can be observed [27], while for concrete-UHPFRC/RC composite beams cracking pattern is not such intense (Fig. 10).

Beams B1 and B2 (type 1) were taken as reference ones and compared to composite beams type 2 and type 3. The influence of 50 mm layer of UHPFRC in tension zone can be explained in such a way. Until the crack opening the curves have similar slope, however at higher loads it has important differences. Several points can be taken for clear explanation. Taking the average values of both type 2 beams, the reduction of composite beams deflection at 60 kN – 37.73%, 80 kN – 30.98%, 100 kN – 30.27% and 120 kN – 27.54%. Furthermore, load bearing capacity is also increased: average yielding load for type 1 beams is about 130.4 kN and failure load 153.89 kN, while for type 2 beams 166.46 kN and 178.21 kN, respectively. Theoretically, UHPFRC layer thickness has influence on member stiffness, however under this experiment conditions it was obtained similar results between beams with 50 mm and 70 mm UHPFRC layers. This could be explained due to possibly different fibre orientation in these members and other possible factors which could be related to behaviour of UHPFRC layer. For type 3 beams the average yielding and ultimate loads are 160.83 kN and 179 kN, respectively.

Middle section of the beams was chosen to determine the strains and stresses in reinforcement experimentally. It was determined during the experiment that not for all beams the first crack opened in the middle section of the beam, where strain gauges were installed, but in other section away from the strain gauges. This influenced on lower reinforcement stress immediately after the crack opening. It can be observed for beams B3 and B4 in Fig. 11. At higher loads, when the crack opened in midspan of the beam the tensile stress of reinforcement is similar.

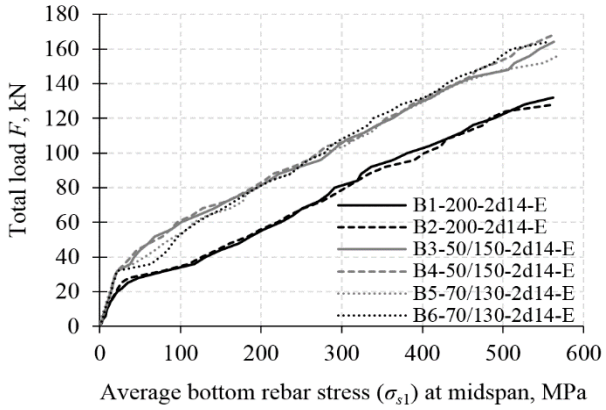

Fig. 11 Total load-stress in tensile rebar stress relation

The same load steps as for deflection analysis can be chosen to compare tensile reinforcement stresses. In this case type 1 and type 3 beams can be compared, because for these beams the first cracks opened in middle section, where strain gauges were installed. Taking B1 and B2 beams as reference ones, the average reduction of tensile stress in B5 and B6 beams bottom reinforcement at 60 kN – 46.37%, 80 kN – 34.46%, 100 kN – 29.07%, 120 kN – 28.09%.

Using measured strain values in bottom and top reinforcement, curvature of all beams were calculated. Results are presented in Fig. 12.

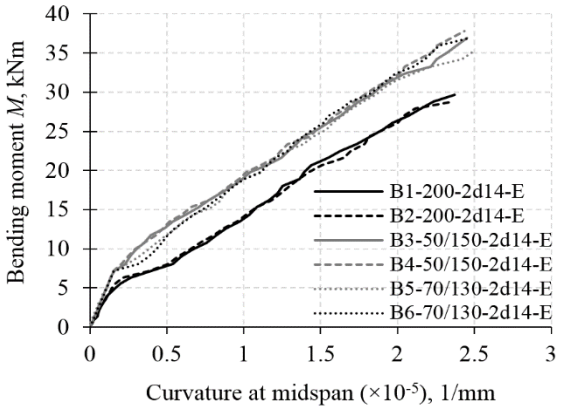

Fig. 12 Experimentally determined curvature at midspan

For composite concrete-UHPFRC/RC flexural members, important role should be paid to interface debonding. However, under this experiment conditions, when new composite beams were made, it was not observed any problems due to interface zone.

4.2. Comparison of experimental and numerical results

4.2.1. General information

Two types of beams were modelled using numerical calculations. Numerically obtained load-deflection relationships of type 2 and type 3 beams were compared with experimental results. As it was mentioned above, tensile strength of UHPFRC has very significant role on structural performance of flexural composite members. It can be measured indirectly from 4-point bending tests on unnotched prisms. However, elastic tensile strength should be corrected from scale and gradient effects (Eq. 4). As it is given in interim recommendations [13] the default value of α number is 0.08 for strain-softening UHPFRC material, and it should be recalibrated for strain-hardening materials. CEB/FIP model code 2010 defines $\alpha = 0.06$ for normal strength concrete and for high strength concrete this number should be replaced by lower than 0.06 value, which has to be determined experimentally. Variety of α number determined to additional inaccuracy of results.

$$f_{ct,el} = f_{ct,fl} \frac{\alpha a^{0.7}}{1+\alpha a^{0.7}}, \quad (4)$$

where a is height of the prism in mm.

Despite the fact that calculating elastic tensile strength from flexural tensile strength, the result is influenced of α number, another significant problem is actual tensile strength in flexural member. For full scale beams steel fibres distribution and orientation over the length of the beam can vary in different sections.

Taking into consideration the facts mentioned above, numerical analysis was made, assuming different tensile strength as variable. Average value of flexural tensile strength, determined from 4-point bending tests is 11.59 MPa. Four different cases were analysed: $\alpha_1 = 0.04$ ($f_{ct,el1} = 5.81$ MPa), $\alpha_2 = 0.06$ ($f_{ct,el2} = 6.97$ MPa), $\alpha_3 = 0.08$ ($f_{ct,el3} = 7.74$ MPa), $\alpha_4 = 0.1$ ($f_{ct,el4} = 8.29$ MPa). In any case, the variety of tensile strength has significant influence on structural behaviour of flexural composite members. In all

figures experimental results are indicated with “E” and numerical results with “N”.

4.2.2. Results of composite beams 50/150-2d14

Four different values of UHPFRC elastic tensile strength were included into analysis. Other mechanical properties were assumed as constant values as it is given in Table 3. As it can be seen from Fig. 13, in all four cases numerically calculated load-deflection relations immediately after crack opening show lower values of deflection in comparison to experimental results. The slope of curves decreases at higher loads and at about yielding strength it shows bigger deflections. Approximate value of G_f fracture energy was chosen equal to 15 N/mm, which could be possible for UHPFRC, higher and lower values were also checked, but under this analysis conditions, the sensitivity of G_f parameter was not observed and comparison with different values is not presented in this study.

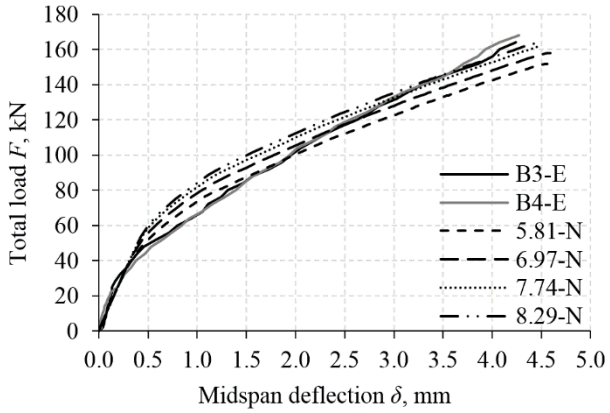

Fig. 13 Numerical versus experimental load-deflection results of composite 50/150-2d14 beams

Tensile stress in bottom reinforcement is determined in quite sufficient range in all four cases (Fig. 14).

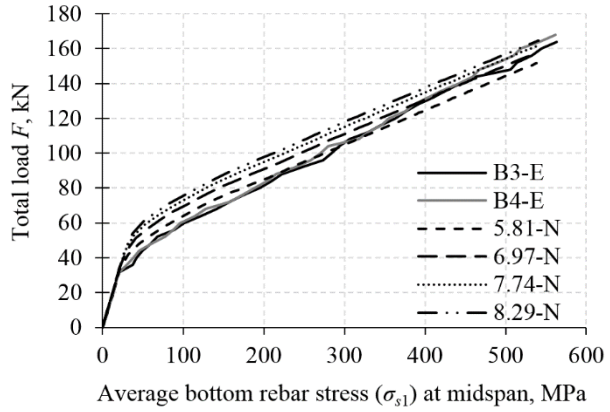

Fig. 14 Numerical versus experimental load-tensile rebar stress relation of composite 50/150-2d14 beams

The main differences observed immediately after the crack opening. The first reason for these inaccuracies is the first crack position over the length of the beam. It can open anywhere in the pure bending zone. Under this experiment conditions strain gauges were fixed in the middle of the beam. The second reason is the influence of material models and FE method. However, the total load at about yielding point is very similar.

Bending moment-curvature relation in the middle span of the beams was also calculated from experimentally obtained results and compared with numerically obtained curvature. Fig 15 shows that difference between experimental and numerical curvature is minimum.

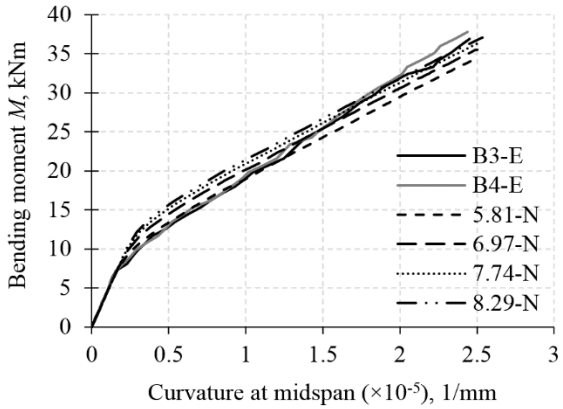

Fig. 15 Numerical versus experimental bending moment-curvature relation of composite 50/150-2d14 beams

4.2.3. Results of composite beams 70/130-2d14

The results of composite beams B5 and B6 have a little bigger inaccuracy comparing experimental and numerical relationships presented below (Figs. 16-18). At first, it should be noted that under this experiment conditions the results of composite beams B5 and B6 were very similar to beams B3 and B4. The explanation of this similarity is given in section 4.1. In numerical model, assuming all mechanical properties and cross-section parameters the same, except UHPFRC layer thickness, undoubtedly has significant influence on structural performance of composite beams. Therefore, higher stiffness of FE curves could be explained not only due to influence of FE model, but also due to many factors (tensile strength of concrete and UHPFRC, cracks distribution, fibres distribution and orientation, etc.) which had influence in experimental results. Load-deflection relation of composite 70/130-2d14 beams are presented below, in Fig. 16.

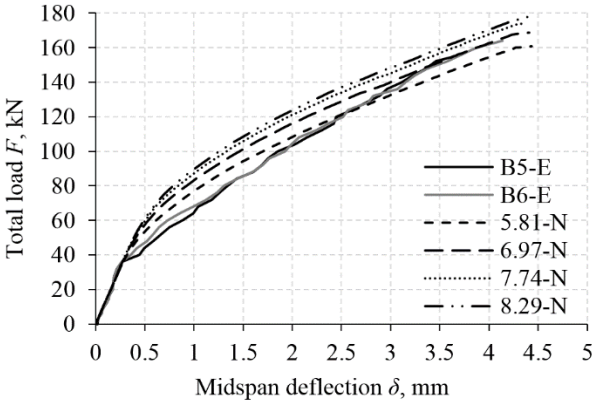

Fig. 16 Numerical versus experimental load-deflection results of composite 70/130-2d14 beams

Due to above mentioned factors tensile stress in bottom reinforcement of B5 and B6 beams is different than it was determined from FE analysis (Fig. 17).

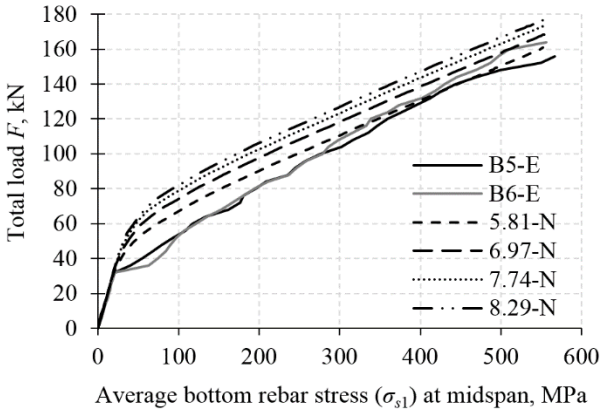

Fig. 17 Numerical versus experimental load-tensile rebar stress relation of composite 70/130-2d14 beams

As for composite beams 50/150-2d14, the same reasons for 70/130-2d14 had negative influence on differences between experimental and numerical results. It also should be noted that material models of UHPFRC (post-failure tensile stress-displacement relation, post-failure tensile stress-fracture energy relation) are limited to describe strain-hardening effect immediately after the crack opening. Using these models strain-hardening of tensile UHPFRC is neglected and after the crack opening the decreasing of strength occurs. Due to this reason it is difficult to represent precise structural behaviour of flexural composite concrete-UHPFRC/RC members.

Bending moment-curvature relation in the middle span of 70/130-2d14 beams are presented in Fig. 18.

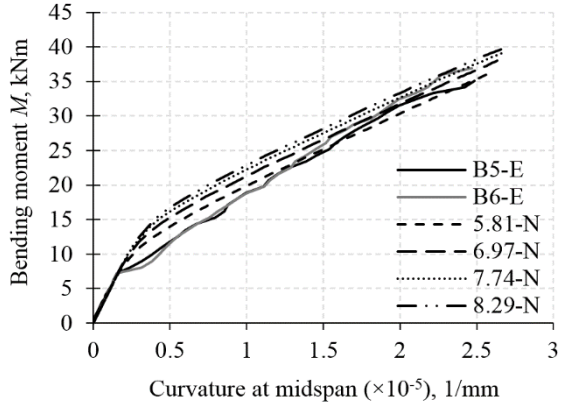

Fig. 18 Numerical versus experimental bending moment-curvature relation of composite 70/130-2d14 beams

5. Conclusions

1. Under carried out experiment conditions, efficiency of newly cast flexural concrete-UHPFRC/RC composite members in comparison to reinforced concrete beams can be described as enhanced flexural capacity, increased stiffness, reduced crack widths and spacing, and reduced reinforcement tensile stress.

2. Similar results between beams with different UHPFRC layers (50 and 70 mm) can be explained by some variety of tensile behaviour of UHPFRC that was fixed in flexural tensile strength tests. However, it was not observed any debonding at interface zone between concrete and UHPFRC.

3. In most cases of FE calculations, the values of deflection, curvature and tensile stress of reinforcement immediately after the crack opening was obtained lower at the same level of loads in comparison to experimental results. However, at higher loads, variation of numerical and experimental values was not uniform. Stiffer behaviour of numerical results partly could be explained due to assumed perfect bond between different materials in FE model. As well as, using post-failure tensile stress-displacement or tensile stress-fracture energy relations, it is not possible to evaluate strain-hardening effect of tensile UHPFRC, and the material model has to be simplified. Analysis of variety of tensile strength showed significant influence on the results of composite beams.

References

1. **Brühwiler, E.; Denarié, E.** 2013. Rehabilitation and strengthening of concrete structures using ultra-high performance fibre reinforced concrete, Structural Engineering International 23(4): 450-457. http://dx.doi.org/10.2749/101686613X13627347100437.
2. **Habel, K.; Denarié, E.; Brühwiler, E.** 2006. Structural response of elements combining ultrahigh-performance fiber-reinforced concretes and reinforced concrete, Journal of Structural Engineering 132(11): 1793-1800. http://dx.doi.org/10.1061/(ASCE)0733-9445(2006)132:11(1793).
3. **Habel, K.** 2004. Structural behaviour of elements combining ultra-high performance fibre reinforced concretes (UHPFRC) and reinforced concrete, PhD thesis, Swiss Federal Institute of Technology, Lausanne, Switzerland.
4. **Lampropoulos, A.P.; Paschalis, S.A.; Tsioulou, O.T.; Dritsos, S.E.** 2016. Strengthening of reinforced concrete beams using ultra high performance fibre reinforced concrete (UHPFRC), Engineering Structures 106: 370-384. http://dx.doi.org/10.1016/j.engstruct.2015.10.042.
5. **Noshiravani, T.; Brühwiler, E.** 2013. Experimental investigation on reinforced ultra-high-performance fibre-reinforced concrete composite beams subjected to combined bending and shear, ACI Structural Journal 110(2): 251-261.
6. **Noshiravani, T.; Brühwiler, E.** 2014. Analytical model for predicting response and flexure-shear resistance of composite beams combining reinforced ultrahigh performance fiber-reinforced concrete and reinforced concrete, Journal of Structural Engineering 140(6): 04014012-1-04014012-10. http://dx.doi.org/10.1061/(ASCE)ST.1943-541X.0000902.
7. **Wuest, J.** 2006. Structural behaviour of reinforced concrete elements improved by layers of ultra high performance reinforced concrete, 6th International PhD Symposium in Civil Engineering, Zurich.
8. **Hussein, L.** 2015. Structural Behaviour of Ultra High Performance Fibre Reinforced Concrete Composite Members. PhD thesis, Department of Civil Engineering, Ryerson University, Toronto, Canada.
9. **Hussein, L.; Amleh, L.** 2015. Structural behavior of ultra-high performance fibre reinforced concrete-normal strength concrete or high strength concrete composite members, Construction and Building Materials 93: 1105-1116.

http://dx.doi.org/10.1016/j.conbuildmat.2015.05.030.
10. EN 1992-1-1:2004. Eurocode 2: Design of Concrete Structures - Part 1-1: General Rules and Rules for Buildings. CEN, Brussels, Oct. 2004
11. Model Code 1990. CEB-FIP. London (UK): Thomas Telford; 1993
12. Fib Model Code for Concrete Structures 2010. CEB-FIP. Berlin (Germany): Ernst & Sohn; 2010
13. AFGC-SETRA. Ultra-high performance fibre-reinforced concretes – Interim recommendations. France; 2013
14. **López, J.Á.; Serna, P.; Navarro-Gregori, J.; Camacho, E.** 2015. An inverse analysis method based on deflection to curvature transformation to determine the tensile properties of UHPFRC, Materials and Structures 48(11): 3703-3718. http://dx.doi.org/10.1617/s11527-014-0434-0.
15. **Graybeal, B.A.** 2014. Tensile mechanical response of ultra-high-performance concrete, Advances in Civil Engineering Materials 4(2): 62-74. http://dx.doi.org/10.1520/ACEM20140029.
16. **Wille, K.; El-Tawil, S.; Naaman, A.E.** 2014. Properties of strain hardening ultra high performance fiber reinforced concrete (UHP-FRC) under direct tensile loading, Cement & Concrete Composites 48: 56-66. http://dx.doi.org/10.1016/j.cemconcomp.2013.12.015
17. **Awinda, K.; Chen, J.; Barnett, S.J.** 2016. Investigating geometrical size effect on the flexural strength of the ultra high performance fibre reinforced concrete using the cohesive crack model, Construction and Building Materials 105: 123-131. http://dx.doi.org/10.1016/j.conbuildmat.2015.12.012.
18. **Chen, L.; Graybeal, B.A.** 2012. Modeling structural performance of ultrahigh performance concrete I-girders, Journal of Bridge Engineering 17(5): 754-764. http://dx.doi.org/10.1061/(ASCE)BE.1943-5592.0000305.
19. Finite Element Analysis of Ultra-High Performance Concrete: Modeling Structural Performance of an AASHTO Type II Girder and a 2nd Generation Pi-Girder. FHWA Publication No. FHWA-HRT-11-020.
20. **Mahmud, G.H.; Yang, Z.; Hassan, A.M.T.** 2013. Experimental and numerical studies on size effects of ultra high performance fibre reinforced concrete (UHPFRC) beams, Construction and Building Materials 48: 1027-1034. http://dx.doi.org/10.1016/j.conbuildmat.2013.07.061.
21. **Lee, J.; Fenves G.L.** 1998. Plastic-damage model for cyclic loading of concrete structures, Journal of Engineering Mechanics 124(8): 892-900.
22. ABAQUS 6.13 Analysis User's Guide Volume III: Materials.
23. **Xu, M.; Wille, K.** 2015. Fracture energy of UHP-FRC under direct tensile loading applied at low strain rates, Composites Part B: Engineering 80: 116-125. http://dx.doi.org/10.1016/j.compositesb.2015.05.031.
24. **Wille, K.; Naaman, A.E.** 2010. Fracture energy of UHP-FRC under direct tensile loading, Proceedings of FraMCoS-7, Seoul.
25. **Demir, A.; Ozturk, H; Dok, G.** 2015. 3D numerical modelling of RC deep beam behaviour by nonlinear finite element analysis, Disaster Science and Engineering 2(1): 13-18.
26. **Sümer, Y.; Aktaş, M.** 2015. Defining parameters for concrete damage plasticity model, Challenge Journal of Structural Mechanics 1(3): 149-155. http://dx.doi.org/10.20528/cjsmec.2015.07.023.
27. **Yang, I.H.; Joh, C.; Kim, B.S.** 2010. Structural behavior of ultra high performance concrete beams subjected to bending, Engineering Structures 32: 3478-3487. http://dx.doi.org/10.1016/j.engstruct.2010.07.017.

T. Zingaila, M. Augonis, M.R.T. Arruda, E. Šerelis, Š. Kelpša

EXPERIMENTAL AND NUMERICAL ANALYSIS OF FLEXURAL CONCRETE-UHPFRC/RC COMPOSITE MEMBERS

S u m m a r y

This paper presents experimental and numerical analysis of newly cast flexural concrete-UHPFRC/RC beams. In total, 4 intermediate-scale composite beams were cast and tested using 4-point bending test setup. Midspan deflection, curvature and reinforcement strains were measured during experimental program. Clear efficiency of composite beams was observed in comparison to RC beams: enhanced flexural capacity, increased stiffness, reduced crack widths and spacing, and reduced reinforcement tensile stress. All experimental results were compared with numerical calculations. Analysis of variety of tensile strength of UHPFRC showed significant influence on the results of composite beams. As well as, using post-failure tensile stress-displacement or tensile stress-fracture energy relations, it is not possible to evaluate strain-hardening effect of tensile UHPFRC, and the material model has to be simplified. However, experimental and numerical results were in sufficiently good agreement.

Keywords: UHPFRC, composite members, ABAQUS.

Received December 07, 2016
Accepted April 14, 2017